

Manipulating the exchange bias effect of $\text{Pb}(\text{Zr}_{0.52}\text{Ti}_{0.48})\text{O}_3/\text{CoFe}_2\text{O}_4/\text{NiO}$ heterostructural films by electric fields

Yong-Chao Li,¹ Dan-Feng Pan,¹ Jun Wu,¹ Ying-bin Li,¹ Guang-hou Wang,^{1,2}
 Jun-Ming Liu,^{1,2} and Jian-Guo Wan^{1,2,a)}

¹National Laboratory of Solid State Microstructures and Department of Physics, Nanjing University,
 Nanjing 210093, China

²Collaborative Innovation Center of Advanced Microstructures, Nanjing University, Nanjing 210093, China

(Received 16 July 2016; accepted 16 October 2016; published online 27 October 2016)

The $\text{Pb}(\text{Zr}_{0.52}\text{Ti}_{0.48})\text{O}_3/\text{CoFe}_2\text{O}_4/\text{NiO}$ heterostructural films with exchange bias (EB) effect have been prepared on Pt/Ti/SiO₂/Si wafers using a sol-gel process, and reversible manipulation of EB effect by electric fields has been realized. Compared with the exchange bias field ($H_{\text{eb}} = -75$ Oe) at as-grown state, the modulation gain of H_{eb} by electric fields can reach 83% ($H_{\text{eb}} = -12.5$ Oe) in the case of +5.0 V and 283% ($H_{\text{eb}} = -287.5$ Oe) in the case of -5.0 V, respectively. Moreover, such electrically tunable EB effect is repeatable and has good endurance and retention. Through analyzing the energy band structures in different electric treatment states, we discuss the mechanism of such electric-field-tunable EB effect. Two factors, i.e., the filling (or releasing) of electrons into (or from) the defect levels produced by oxygen vacancies at positive (or negative) electric voltages, and the redistribution of electrons due to the ferroelectric polarization, both of which give rise to the variation of the strength of exchange interaction in the CFO layer, have been revealed to be responsible for the electric modulation of EB effect. This work provides a promising avenue for electrically manipulating the EB effect and developing high-performance memory and storage devices with low power consumption. *Published by AIP Publishing.* [<http://dx.doi.org/10.1063/1.4966545>]

Exchange bias (EB) effect has great applications on the fabrication of spin-valves and magnetic tunnel junctions,¹⁻³ and it has been the research highlight in magnetic data storage and spintronic fields in the past few years.⁴⁻⁸ It is generally accepted that the EB effect originates from exchange coupling of the spins in the ferromagnetic (FM) to uncompensated pinned spins in antiferromagnetic (AFM) at the FM/AFM interface.⁹⁻¹¹ It manifests itself as a shift of the magnetic hysteresis loop along the fixed field axis. The shift, measured by exchange bias field (H_{eb}), appears after cooling the EB system under an external magnetic field down through the Néel temperature (T_{N}) of the AFM part. Tunable EB effect shows great value in actual applications.⁶⁻⁸ For this purpose, various approaches have been explored and tunable EB effect has been realized in some material systems.¹²⁻¹⁸ Among them, the switching of EB effect by magnetoelectric coupling is a promising way, which has been demonstrated in $\text{Cr}_2\text{O}_3(111)/(\text{Co}/\text{Pt})_3$ system despite the fact that the switching is elusive at room temperature and needs complicated procedures.¹²⁻¹⁴ Nevertheless, the recent advent of boron-doped Cr_2O_3 with decisively enhanced Néel temperature (~ 400 K at 3% boron doped at oxygen sites) makes the realization of electrically tunable EB effect in such system become facile and provides a possibility for commercial applications.¹⁵ Another feasible avenue is to control the photo-carrier using light irradiation in the multiferroic heterostructure such as $\text{BiFeO}_3/\text{La}_{2/3}\text{Sr}_{1/3}\text{MnO}_3$ thin films.¹⁶ But in this case, the modulation is volatile because the photo-injected electrons will vanish when the light irradiation is

removed. Full electric field control of EB effect may be an alternative approach, which has been achieved in some BiFeO_3 -based heterostructure.^{17,18} Nevertheless, the manipulation is irreversible or needs low temperature condition, which limits its actual applications.

It is known that the EB effect belongs to the interface coupling, and the value of H_{eb} is closely correlated to the properties of FM and AFM components, including the saturated magnetization (M_{s}), the thickness, the anisotropy, and so on.^{10,11} If these properties can be modulated, the tunable EB effect may be expected. Herein, we propose a route to achieve the electric-tunable EB effect at room temperature by constructing a tri-layer heterostructure composed of ferroelectric (FE), ferrimagnetic (FIM), and AFM layers. Thanks to the introduction of FE layer, it becomes possible to modulate the magnetism of FIM layer by external electric fields via the interfacial coupling and further change the magnetic exchange coupling between the FIM and AFM layers.¹⁹⁻²¹ Accordingly, the electric manipulation of H_{eb} in such tri-layer heterostructure may be realized.

In this letter, we report on a remarkable electric manipulation of EB effect at room temperature in a tri-layer heterostructural film stacked sequentially by $\text{PZT}(\text{Zr}_{0.52}\text{Ti}_{0.48})\text{O}_3$ (PZT, FE layer), CoFe_2O_4 (CFO, FIM layer), and NiO (AFM layer). Great change in EB effect is observed after the electric treatments. The gain in increasing H_{eb} can reach 83% in the case of +5.0 V treatment, while 283% in the case of -5.0 V treatment. Moreover, we demonstrate that such electric-field-tunable EB effect is repeatable and has good endurance and retention. Through analyzing the change in the energy band structures under different electric fields, we reveal the mechanism of electrically manipulating EB effect

^{a)}Author to whom correspondence should be addressed. Electronic mail: wanjg@nju.edu.cn

that originates from the change in the magnetization of FIM layer due to the coupling between the FE and FIM layers.

The PZT/CFO/NiO film was prepared by a sol-gel process and spin coating technique. The NiO, CFO, and PZT layers in turn were grown on the Pt/Ti/SiO₂/Si(100) wafer. Before depositing the next layer, each layer was dried at 280 °C for 10 min and then annealed at 650 °C for 5 min by a rapid annealing process under oxygen atmosphere. The details of the preparation can be found elsewhere.²² In order to induce the EB effect, we subsequently treated the film by a field cooling process as follows: The film was first heated to 350 °C, and then was cooled gradually to room temperature under an in-plane 2000 Oe DC magnetic field. For electric measurements, 100 nm-thick Au top electrodes with 1.0 mm in diameter were finally deposited onto the surface of the film using ion sputtering technique.

The phase structures of the film were analyzed by X-ray diffraction (XRD) on a D/MAXRD diffractometer using Cu K α radiation, as shown in Figure 1(a). The film consists of perovskite PZT, spinel CFO and rock-salt NiO phases. Besides, no other impure phase is observed. The cross-sectional scanning electron microscopy (SEM) image of the film was carried out using a scanning electron microscopy (SEM, LEO-1530VP), as shown in the inset of Figure 1(a). The upper PZT layer, middle CFO layer, and bottom NiO layer are about 100 nm, 30 nm, and 40 nm in thickness, respectively. Figure 1(b) presents the ferroelectric hysteresis loop measured by a standard ferroelectric test system (Precision Multiferoic, Radiant, Inc.). The film exhibits evident ferroelectric hysteresis characteristics with the remanent

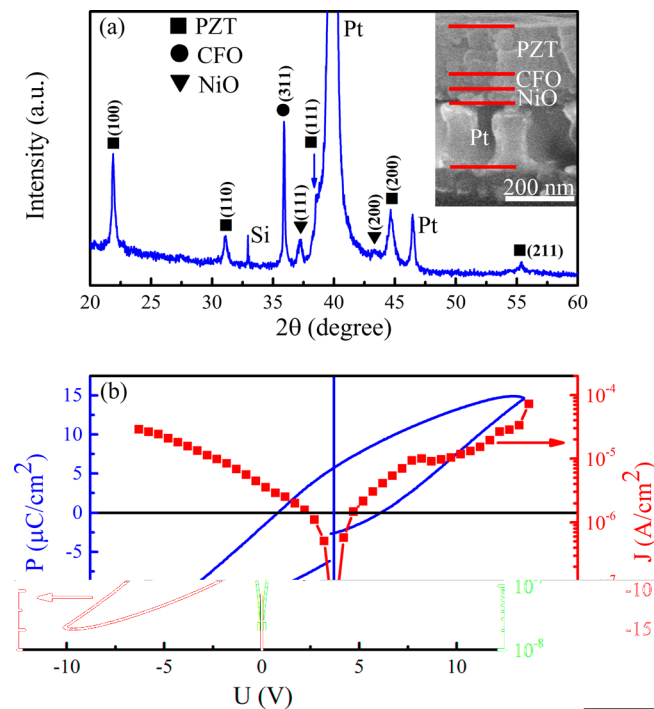


FIG. 1. (a) XRD patterns of the PZT/CFO/NiO film. The inset is the corresponding cross-sectional SEM image. (b) Ferroelectric polarization vs. voltage (P-U) loop (the blue solid line) and the current density vs. voltage (J-V) curve (the red line with solid squares). For the measurements of P-U loop, a standard bipolar triangular waveform with a measuring frequency of 10 kHz was used. The J-V curve was measured with a 0.5 V sweeping step from -10.0 V to $+10.0$ V.

polarization $2P_r \sim 12.0 \mu\text{C}/\text{cm}^2$ and ferroelectric coercive voltage $V_c \sim 2.9$ V. Figure 1(b) also gives the current density (J) vs. voltage curve recorded by an ampere meter (Keithley 6517B). The leakage current is quite low (typically, only $\sim 1 \times 10^{-4}$ A/cm² at ± 10.0 V), indicative of good insulating property. The in-plane magnetization vs. magnetic field (M-H) curve of the as-grown film was measured at room temperature on a superconducting quantum interference device magnetometer (VSM-SQUID, Quantum Design), as shown in the green curve with solid squares of Figure 2. The as-grown film exhibits well-defined ferromagnetic characteristics with distinguished EB effect. The M_s and H_{eb} values are $175 \text{ emu}/\text{cm}^3$ and -75 Oe, respectively.

For the present tri-layer heterostructure, it is possible to manipulate the EB effect by electric fields since the EB effect originates from the exchange interaction at the CFO/NiO interface while the coupling between CFO and PZT can provide us a chance to tune the magnetism of CFO by the ferroelectric polarization of PZT. To verify this, we made the electric treatments on the films and then carried out the measurements of M-H loops to observe the change in magnetic features. The electric treatment process was carried out as follows: An electric voltage was applied to the film for 10 ms on a Keithley 2400 system, and then removed. The applied electric voltage was set to $+5.0$ V or -5.0 V, which exceeded the ferroelectric coercive voltage of the film so that the ferroelectric domain in PZT layer can be reversed adequately. Figure 2(a) presents typical room-temperature M-H loops after the film was treated by $+5.0$ V and -5.0 V electric voltages. One observes that after being subject to electric treatments, the film has an evident change in the M_s value. In the case of $+5.0$ V treatment, the film has a $\sim 24\%$ gain in increasing the M_s value, i.e., from 175 to $217 \text{ emu}/\text{cm}^3$. On the contrary, after being treated by -5.0 V electric voltage, the film has a 36% drop in the M_s value, decreasing from

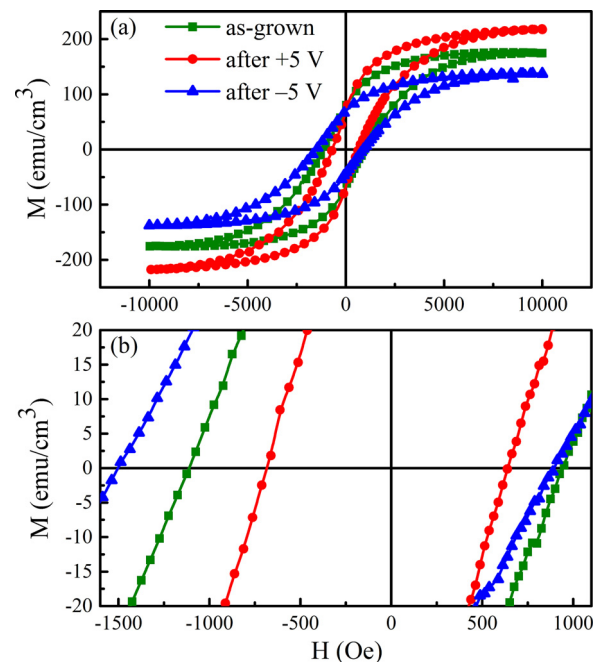


FIG. 2. (a) In-plane magnetization vs. magnetic field (M-H) loops of the PZT/CFO/NiO film at as-grown state, $+5.0$ V and -5.0 V treatment states. (b) Enlarged curves of Figure 2(a).

217 to 137 emu/cm^3 . More interestingly, the EB effect varies greatly with the variation of magnetization. From the enlarged curves in Figure 2(b), one observes a remarkable left shift of M-H loops whether the film is treated by $+5.0 \text{ V}$ or -5.0 V . Based on the Equation (S4) shown in the [supplementary material](#), we calculated the H_{eb} values for different electric treatment states, i.e., $H_{\text{eb}} = -75 \text{ Oe}$ for the as-grown state, $H_{\text{eb}} = -12.5 \text{ Oe}$ for the $+5.0 \text{ V}$ treatment state (83% gain), and $H_{\text{eb}} = -287.5 \text{ Oe}$ for the -5.0 V treatment state (283% gain). See more data in Section I of the [supplementary material](#). These results indicate that the EB effect can be well manipulated by electric fields, even if electric fields are removed.

Repeatability and stability of such electric-field-tunable EB effect are important for actual applications. To examine them, we repeatedly treated the films by alternately applying $+5.0 \text{ V}$ and -5.0 V electric voltages and then measured the dependence of M_s and H_{eb} on the cycling number, as shown in Figure 3(a). One observes that after the film is subject to several cycling treatments by $+5.0 \text{ V}$ or -5.0 V electric voltages, both M_s and H_{eb} almost have no change. On the other hand, from the dependence of M_s and H_{eb} on aging time as shown in Figure 3(b), we find that the electrical manipulation of EB effect is also quite stable. Even after 30 days, the film treated by $+5.0 \text{ V}$ still keeps $M_s = 210 \text{ emu/cm}^3$ and $H_{\text{eb}} = -18 \text{ Oe}$, while $M_s = 132 \text{ emu/cm}^3$ and $H_{\text{eb}} = -278 \text{ Oe}$ in the case of -5.0 V , all of which only have a slight drop compared with the initial values. We suggest that such slight drop of M_s value may be attributed to the slight depolarization in the PZT layer. All the above results show that the present electric manipulation of EB effect is nonvolatile and stable.

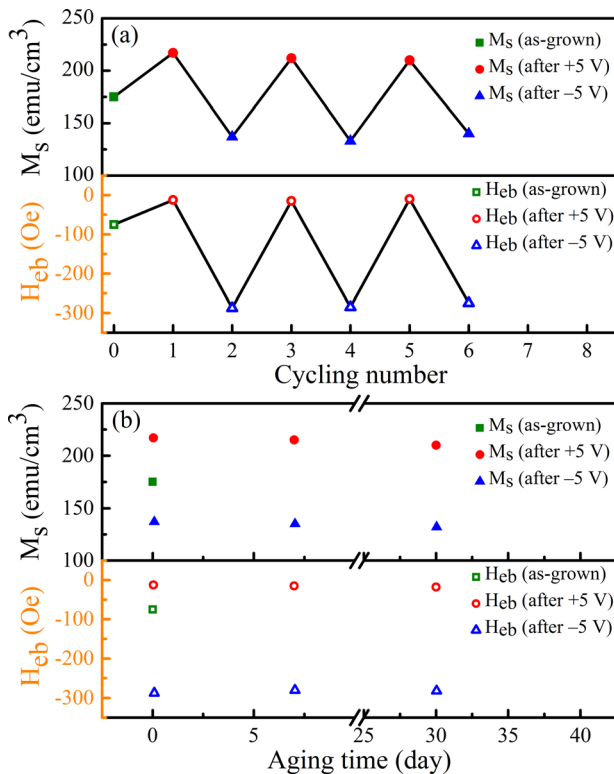


FIG. 3. (a) The dependence of M_s and H_{eb} on the cycling number of alternatively applying $+5.0 \text{ V}$ and -5.0 V . (b) The dependence of M_s and H_{eb} on aging time.

The electric manipulation of EB effect in the present tri-layer film is different from previous methods.^{12–19} In previous investigations, the modulation of H_{eb} was realized by changing the magnetic structures of AFM layer (e.g., in the Cr_2O_3 -based and BiFeO_3 -based systems)^{12–18} or changing the easy axis direction of FM layer (e.g., in the AFM/FeGaB/PZN-PT system).¹⁹ Differently, for the present film, the modulation of H_{eb} is realized by changing the value of M_s . Compared with the gigahertz compatible EB devices (e.g., MERAM bases on chromia-CoPt multilayers),^{14,15} although the switching rate of EB effect in the present heterostructures is slow (only 10^2 s^{-1}), we believe that it can be further improved based on the unique dynamical process (See detailed analyses in Section III of the [supplementary material](#)).^{23,24} Besides, due to good insulating property (see Figure 1(b)), the power consumption used to tune the EB effect is quite low. For example, if the area of the device cell is $10^4 \mu\text{m}^2$, the power will be only $\sim 10^{-8} \text{ W}$, which is low enough for reducing the actual power consumption and helpful to improve the thermal stability of the devices.

We now turn to explore the mechanism of electrically manipulating the EB effect. From Figure 2, a distinct correlation between H_{eb} and M_s is observed, i.e., with M_s decreasing, H_{eb} increases, and vice versa. Accordingly, we consider that the modulation of M_s in the CFO layer should play a crucial role in tuning the EB effect. It is known that CFO has an AB_2O_4 molecular formula in which both spinel structure and inverse spinel structure coexist. Two indirect exchange interactions, i.e., double exchange and superexchange, simultaneously exist and produce a FIM structure.^{25–27} These two exchange interactions in CFO must go via the media, i.e., the electrons from the oxygen atoms in the $\text{Fe}^{3+}\text{-O}^{2-}\text{-Fe}^{3+}$, $\text{Fe}^{3+}\text{-O}^{2-}\text{-Co}^{2+}$, and $\text{Co}^{2+}\text{-O}^{2-}\text{-Co}^{2+}$ chains.^{24,25} Nevertheless, since oxygen vacancies are inevitably produced in CFO during the fabrication process, the strength of the two exchange interactions is actually lower than the ideal value. In this sense, the magnetism of the CFO layer is seriously influenced by the electron states of oxygen vacancies.^{24,28,29}

In the present tri-layer heterostructure, the introduction of PZT layer provides us a feasible avenue to tune the magnetism of CFO layer by electric fields. Figure S2 in the [supplementary material](#) presents the capacitance vs. frequency curves for the PZT/CFO/NiO films treated by $+5.0 \text{ V}$ and -5.0 V . One clearly observes that the capacitance value of the film treated by $+5.0 \text{ V}$ is much larger than that of the film treated by -5.0 V , indicative of the existence of ferroelectric polarization in the PZT layer. Such ferroelectric polarization not only can change the band structure of the whole heterostructure, but also can induce an interfacial coupling between PZT and CFO layers, both of which make it possible to tune the electronic state of oxygen vacancies in CFO (See detailed analyses in Section II of the [supplementary material](#)).²⁴ To understand the role of PZT in tuning the magnetic and electronic states of the whole heterostructure, we illustrated the schematic diagrams of the energy band structure for the PZT/CFO/NiO film at different electric treatment states, as shown in Figure 4. We first analyze the case of $+5.0 \text{ V}$ shown in Figure 4(b). When a $+5.0 \text{ V}$ electric voltage is applied to the film, the electrons move from Au to Pt electrode, nevertheless, due to high potential barrier at

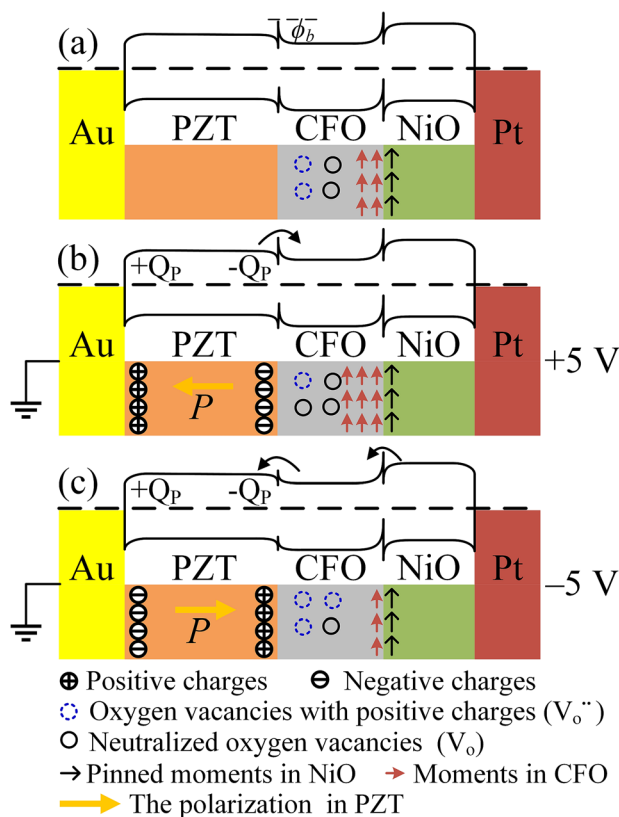


FIG. 4. Schematic diagrams of the energy band structures of the PZT/CFO/NiO film at various states (a) initial state, (b) +5.0 V treatment state, (c) -5.0 V treatment state.

CFO/NiO interface, most electrons cannot pass through the CFO/NiO interface and part of them are trapped by the defect energy level of oxygen vacancies in CFO. As a result, part of positively charged oxygen vacancies (V_{O}^{\bullet}) in CFO are neutralized by these trapped electrons, so the strength of exchange interactions between the Fe/Co ions increases due to the increased electrons acting as exchange interaction media. On the other hand, after the electric voltage is removed, due to the ferroelectric polarization in PZT, negative polarization charges gather at the PZT/CFO interface. So the V_{O}^{\bullet} in CFO tend to move towards the PZT/CFO interface, while the electrons gathering at the interface move away, and part of them are trapped by the V_{O}^{\bullet} in the interior of the CFO layer. This causes the number of electrons taking part in the exchange interaction to further increase. So the magnetic exchange interaction in the whole CFO layer becomes strong, which brings about an increased M_s value, as shown in Figure 2(a).

The situation becomes different when the film is subject to -5.0 V. As shown in Figure 4(c), since the direction of ferroelectric polarization in PZT changes completely, the potential barrier height ϕ_b at PZT/CFO interface decreases.^{30,31} So part of electrons trapped by V_{O}^{\bullet} in the CFO layer is released and pass through the CFO/PZT interface. As a result, the number of electrons trapped by V_{O}^{\bullet} in the CFO layer decreases and part of oxygen vacancies return back to the positively charged state. In addition, the reversed ferroelectric polarization in PZT causes an enrichment of positive polarization charges at the PZT/CFO interface, which promotes the oxygen vacancies previously assembling at the PZT/CFO interface to move away and enter into the interior of the CFO

layer. This causes the number of electrons taking part in the exchange interaction to further decrease. Therefore, the magnetic exchange interaction strength in CFO becomes weak, causing a decrease in M_s .

The variation of magnetization in the CFO layer further gives rise to a change in the EB effect of the whole heterostructure. In the present system, both the direction and the value of uncompensated pinned moments in the NiO layer have no change after the heterostructure is subject to the electric treatments. According to Equation S5 shown in the [supplementary material](#), the value of H_{eb} is approximately inversely proportional to the M_s value,^{10,11,32,33} i.e., with increasing the M_s , the H_{eb} reduces, and vice versa. To understand this process, we take an example of the case of +5.0 V treatment. The +5.0 V treatment can cause the electrons to be trapped by the V_{O}^{\bullet} in CFO, which enhances the magnetic exchange interaction. So the moments in CFO having no exchange interaction with uncompensated moments in NiO increase, leading to a weakened EB effect. The contrary is the case of -5.0 V treatment. See detailed analysis in Section III of the [supplementary material](#).

In conclusion, we have realized a reversible manipulation of EB effect by electric fields in the PZT/CFO/NiO films. Both M_s and H_{eb} can be greatly tuned by electric fields. We have also demonstrated that such electric-field-tunable EB effect has good endurance and retention, and that the introduction of FE layer plays an important role in tuning the EB effect. Two factors, i.e., the filling (or releasing) of electrons into (or from) the V_{O}^{\bullet} at positive (or negative) electric voltages, and the redistribution of electrons caused by the interfacial coupling between FE and FIM layers, both of which give rise to the variation of the strength of exchange interactions in FIM, are crucial in manipulating the EB effect. This work provides a promising avenue to realize electric-field-tunable EB effect and exhibits valuable potentials for developing memory and storage devices with low power consumption.

See [supplementary material](#) for more magnetic data, the capacitance data, and the analysis about the process of electrically manipulating EB effect of the PZT/CFO/NiO films.

This work was supported by the National Key Projects for Basic Research of China (Grant No. 2015CB921203), the National Key Research Programme of China (Grant No. 2016YFA0201004), and the National Natural Science Foundation of China (Grant Nos. 51472113 and 11134005).

¹B. Dieny, V. S. Speriosu, S. S. P. Parkin, B. A. Gurney, D. R. Wilhoit, and D. Mauri, *Phys. Rev. B* **43**, 1297 (1991).

²T. Miyazaki and N. Tezuka, *J. Magn. Magn. Mater.* **139**, L231 (1995).

³J. S. Moodera, L. R. Kinder, T. M. Wong, and R. Meservey, *Phys. Rev. Lett.* **74**, 3273 (1995).

⁴V. Skumryev, S. Stoyanov, Y. Zhang, G. Hadjipanayis, D. Givord, and J. Nogués, *Nature* **423**, 850 (2003).

⁵J. Nogués, J. Sort, V. Langlais, V. Skumryev, S. Suriñach, J. S. Muñoz, and M. D. Baró, *Phys. Rep.* **422**, 65 (2005).

⁶M. Bibes and A. Barthelemy, *Nat. Mater.* **7**, 425 (2008).

⁷E. Y. Tsymlal, *Nat. Mater.* **11**, 12 (2012).

⁸M. M. Vopson, *Crit. Rev. Solid State Mater. Sci.* **40**, 223 (2015).

⁹W. H. Meiklejohn and C. P. Bean, *Phys. Rev.* **102**, 1413 (1956); **105**, 904 (1957).

¹⁰J. Nogués and I. K. Schuller, *J. Magn. Magn. Mater.* **192**, 203 (1999).

- ¹¹A. E. Berkowitz and K. Takano, *J. Magn. Magn. Mater.* **200**, 552 (1999).
- ¹²P. Borisov, A. Hochstrat, X. Chen, W. Kleemann, and C. Binek, *Phys. Rev. Lett.* **94**, 117203 (2005).
- ¹³X. Chen, A. Hochstrat, P. Borisov, and W. Kleemann, *Appl. Phys. Lett.* **89**, 202508 (2006).
- ¹⁴X. He, Y. Wang, N. Wu, A. N. Caruso, E. Vescovo, K. D. Belashchenko, P. A. Dowben, and C. Binek, *Nat. Mater.* **9**, 579 (2010).
- ¹⁵M. Street, W. Echtenkamp, T. Komesu, S. Cao, P. A. Dowben, and Ch. Binek, *Appl. Phys. Lett.* **104**, 222402 (2014).
- ¹⁶K. D. Sung, T. K. Lee, Y. A. Park, N. Hur, and J. H. Jung, *Appl. Phys. Lett.* **104**, 252407 (2014).
- ¹⁷Q. Y. Xu, Z. Y. Xu, M. C. He, Y. Q. Cao, and J. Du, *J. Appl. Phys.* **117**, 17D707 (2015).
- ¹⁸S. M. Wu, S. A. Cybart, D. Yi, J. M. Parker, R. Ramesh, and R. C. Dynes, *Phys. Rev. Lett.* **110**, 067202 (2013).
- ¹⁹M. Liu, J. Lou, S. D. Li, and N. X. Sun, *Adv. Funct. Mater.* **21**, 2593 (2011); M. Liu, B. M. Howe, L. Grazulis, K. Mahalingam, T. Nan, N. X. Sun, and G. J. Brown, *Adv. Mater.* **25**, 4886 (2013).
- ²⁰S. Zhang, Y. G. Zhao, P. S. Li, J. J. Yang, S. Rizwan, J. X. Zhang, J. Seidel, T. L. Qu, Y. J. Yang, Z. L. Luo, Q. He, T. Zou, Q. P. Chen, J. W. Wang, L. F. Yang, Y. Sun, Y. Z. Wu, X. Xiao, X. F. Jin, J. Huang, C. Gao, X. F. Han, and R. Ramesh, *Phys. Rev. Lett.* **108**, 137203 (2012); S. Zhang, Y. G. Zhao, X. Xiao, Y. Z. Wu, S. Rizwan, L. F. Yang, P. S. Li, J. W. Wang, M. H. Zhu, H. Y. Zhang, X. Jin, and X. Han, *Sci. Rep.* **4**, 3727 (2014).
- ²¹C. A. Vaz, J. Hoffman, Y. Segal, J. W. Reiner, R. D. Grober, Z. Zhang, C. H. Ahn, and F. J. Walker, *Phys. Rev. Lett.* **104**, 127202 (2010); C. A. F. Vaz, Y. Segal, J. Hoffman, R. D. Grober, F. J. Walker, and C. H. Ahn, *Appl. Phys. Lett.* **97**, 042506 (2010).
- ²²J. G. Wan, X. W. Wang, Y. J. Wu, M. Zeng, Y. Wang, H. Jiang, W. Q. Zhou, G. H. Wang, and J. M. Liu, *Appl. Phys. Lett.* **86**, 122501 (2005).
- ²³J. Li, B. Nagaraj, H. Liang, W. Cao, C. H. Lee, and R. Ramesh, *Appl. Phys. Lett.* **84**, 1174 (2004).
- ²⁴Q. W. Wang, Y. D. Zhu, X. L. Liu, M. Zhao, M. C. Wei, F. Zhang, Y. Zhang, B. L. Sun, and M. Y. Li, *Appl. Phys. Lett.* **107**, 063502 (2015).
- ²⁵J. A. Moyer, C. A. F. Vaz, E. Negusse, D. A. Arena, and V. E. Henrich, *Phys. Rev. B* **83**, 035121 (2011); J. A. Moyer, C. A. F. Vaz, D. A. Arena, D. Kumah, E. Negusse, and V. E. Henrich, *ibid.* **84**, 054447 (2011).
- ²⁶C. M. Srivastava, G. Srinivasan, and N. G. Nanadikar, *Phys. Rev. B* **19**, 499 (1979).
- ²⁷D. Fritsch and C. Ederer, *Phys. Rev. B* **86**, 014406 (2012).
- ²⁸G. Hassnain Jaffari, A. K. Rumaiz, J. C. Woicik, and S. Ismat Shah, *J. Appl. Phys.* **111**, 093906 (2012).
- ²⁹W. Hu, N. Qin, G. H. Wu, Y. T. Lin, S. W. Li, and D. H. Bao, *J. Am. Chem. Soc.* **134**, 14658 (2012).
- ³⁰Z. Wen, C. Li, D. Wu, A. D. Li, and N. B. Ming, *Nat. Mater.* **12**, 617 (2013).
- ³¹Y. B. Lin, Z. B. Yan, X. B. Lu, Z. X. Lu, M. Zeng, Y. Chen, X. S. Gao, J. G. Wan, J. Y. Dai, and J. M. Liu, *Appl. Phys. Lett.* **104**, 143503 (2014).
- ³²J. Stöhr, H. C. Siegmann, M. Cardona, P. Fulde, K. von Klitzing, R. Merlin, H. J. Queisser, and H. Störmer, *Magnetism: From Fundamentals to Nanoscale Dynamics* (Springer, Berlin, Heidelberg, New York, 2006), p. 620.
- ³³H. Ohldag, A. Scholl, F. Nolting, E. Arenholz, S. Maat, A. T. Young, M. Carey, and J. Stohr, *Phys. Rev. Lett.* **91**, 017203 (2003).